NASA TECHNICAL NOTE

NASA TN D-4164

c. 1

LOAN COPY: AFWL
KIRTLAND AFB, N. M.

TECH LIBRARY KAFB, NM
0130705

NASA TN D-4164

ESTIMATES OF LOCAL AND AVERAGE FUEL TEMPERATURES IN A GASEOUS NUCLEAR ROCKET ENGINE

by Albert F. Kascak

Lewis Research Center
Cleveland, Ohio

NATIONAL AERONAUTICS AND SPACE ADMINISTRATION • WASHINGTON, D. C. • SEPTEMBER 1967

TECH LIBRARY KAFB, NM

0130705

NASA TN D-4164

ESTIMATES OF LOCAL AND AVERAGE FUEL TEMPERATURES IN A GASEOUS NUCLEAR ROCKET ENGINE

By Albert F. Kascak

Lewis Research Center
Cleveland, Ohio

NATIONAL AERONAUTICS AND SPACE ADMINISTRATION

For sale by the Clearinghouse for Federal Scientific and Technical Information
Springfield, Virginia 22151 – CFSTI price $3.00

ESTIMATES OF LOCAL AND AVERAGE FUEL TEMPERATURES IN A GASEOUS NUCLEAR ROCKET ENGINE

by Albert F Kascak
Lewis Research Center

SUMMARY

A diffusion analysis is presented of the radiant heat transfer from a centrally located cylinder of gaseous nuclear fuel to a surrounding annulus of flowing hydrogen. The specific reactor analyzed had a cavity length of 6 feet (1.83 m), a cavity diameter of 8 feet (2.44 m), and a fuel diameter of 3.2 feet (0.975 m). Results are shown as radial temperature profiles and integrated average temperatures in the fuel region. Parametric calculations are presented to show the influence on fuel temperature of boundary conditions, radial fuel profiles, fuel ionization and density profiles, the fuel absorption coefficient, reactor pressure, and engine thrust. All calculations are for a specific impulse of 1500 seconds; engine thrust is varied from 10^5 to 10^6 pounds (4.45×10^5 to 4.45×10^6 N), which corresponds to reactor powers from 4 000 to 40 000 megawatts. Most results are presented for a thrust of 500 000 pounds (2.22×10^6 N) and a reactor pressure of 500 atmospheres (5.07×10^7 N/m^2), but a final set of average fuel temperatures are also presented for pressures of 100, 500, and 1000 atmospheres (1.01×10^7, 5.07×10^7, and 10.1×10^7 N/m^2) and a thrust ranging from 10^5 to 10^6 pounds (4.45×10^5 to 4.45×10^6 N).

For a given engine configuration, thrust, specific impulse, and power level, it is shown that boundary conditions of fuel zone edge location and fuel temperature do not significantly affect the average fuel temperature. Fuel ionization and perfect gas density variation with local temperature are likewise relatively unimportant influences on either internal or average fuel temperatures. Using a radially decreasing fuel mole fraction profile in place of a constant radial fuel mole fraction distribution reduces the average fuel temperature from 107 000° to 93 000° R (59 000° to 51 700° K). When the absorption coefficient was increased or decreased by a factor of 10, there was a corresponding increase or decrease in average fuel temperature of about 35 percent.

An increase in reactor pressure or engine thrust caused a significant increase in the average fuel temperature. When all the effects considered were included simultaneously, estimated average fuel temperatures varied from a low of 55 000° R (30 500° K) at 100 atmospheres (1.01×10^7 N/m^2) of pressure and 10^5 pounds (4.45×10^5 N) of thrust to a high of 110 000° R (61 100° K) at 1000 atmospheres (1.01×10^8 N/m^2) of pressure and 10^6 pounds (4.45×10^6 N) of thrust. These results include only the influence of radiative transfer; a significant degree of turbulent heat transport or electron conduction would decrease estimated fuel temperatures.

INTRODUCTION

A number of nuclear rocket propulsion ideas are being considered as ways of producing higher enthalpy hydrogen than can be produced by a solid-core engine. There is insufficient understanding of the basic mechanisms involved to permit a rigorous evaluation of the feasibility of a given concept. Some research studies underway to provide necessary information are described in reference 1. For a gaseous-fueled reactor, the objective of fluid mechanics studies is to be able to predict the velocity and mole fraction distributions that will exist as the hydrogen propellant and nuclear fuel interact in the reactor cavity. Heat-transfer studies are necessary to predict temperature and heat flux distributions within the engine. Average fuel temperature is particularly important because reactor pressure is virtually proportional to it. It is the purpose of this report to describe an analysis of radiative heat transfer in the fuel region of a gas-core reactor. The influence of important variables on both local temperatures, as well as average fuel temperatures will be shown for a range of reactor pressures and thrust levels.

Some previous studies have estimated fuel temperatures with varying degrees of approximation. Reference 2 presents some radiative heat-transfer results using a transport analysis limited to a constant, temperature-independent, gray-gas absorption coefficient. Reference 3 describes a two-dimensional transport solution that considers a gray-gas absorption coefficient that can be both region and temperature dependent. The transport solutions described in references 2 and 3 require computerized numerical techniques to carry out a double integration in the radial and axial directions. If the gas involved is quite opaque, the number of increments required can lead either to excessive machine time or inaccurate answers. This is exactly the situation in the fuel region of a gaseous reactor. The mean free path of thermal radiation in gaseous uranium (ref. 4) is in the range of 1/1000 to 1/10 000 of a foot (0.305 to 0.0305 mm) at densities encountered in gaseous reactors. For a typical physical dimension of 4 feet (1.22 m), the uranium region has an optical diameter from 4 000 to 40 000 photon mean free paths. A "mean free path" is used here as the distance in which radiant flux is decreased to 1/e of its initial value.

It has been suggested (ref. 5) that a diffusion approximation to the transport equation should be used to circumvent this problem. Some preliminary estimates of fuel temperatures obtained with diffusion theory are presented in reference 5. The results reported herein were obtained by extending the basic one-dimensional diffusion analysis to include a number of additional factors not considered in reference 5. Reference 6 has shown that a diffusion analysis with a jump boundary condition is applicable throughout the fueled region.

There are several approximations that can be made in applying a diffusion analysis to gaseous reactor conditions, and it is not clear how strongly these assumptions affect

the calculated fuel temperature. Each of eight variables is investigated - first individually, and then all together. The importance of the variables is shown in terms of their influence on either (1) the local fuel temperature, shown as a radial profile, or (2) the average fuel temperature obtained by radially integrating a mass-weighted temperature profile.

The sensitivity of fuel temperature to the following factors was studied:

(1) Temperature dependence of the absorption coefficient

(2) Radial variation of fuel mole fraction

(3) Perfect gas density variation with temperature

(4) Fuel ionization

(5) Reactor pressure

(6) Boundary values of edge temperature and edge location

(7) Value of the absorption coefficient

(8) Engine thrust level

The inclusion of these variations necessitates information from previous studies. Estimates of uranium opacity were taken from reference 4. Hydrogen opacity was obtained from reference 7. A radial variation of fuel due to mixing with the surrounding hydrogen was obtained by applying the analytical method of reference 8 to typical reactor conditions. Uranium species concentrations as functions of temperature and pressure were obtained from the computer program described in reference 9, which was modified to include charged particles. Uranium ionization potentials necessary for this calculation were provided by the authors of reference 10, while related calculations are discussed in reference 11.

With this information, calculations were carried out to answer two basic questions. First, what is the magnitude of average fuel temperatures to be encountered in a gaseous-fueled reactor, and second, what aspects of the radiative heat transfer process are important in determining fuel temperature? Although the calculations require some specific numerical choices, such as fuel region radius, it is felt that these choices would apply to most, if not all, gaseous reactor concepts.

SYMBOLS

A constant defined in eq. (29)

A' constant defined in eq. (34b)

a_R Rosseland mean absorption coefficient, 1/ft; 1/m

C mole fraction, atoms of fuel/total atoms

K conductivity, (Btu)(ft)/(ft^2)(sec)($^\circ$R); J/(m)(sec)($^\circ$K)

m constant used in curve fit of fuel absorption coefficients

n index used in sum or constant used in curve fit of fuel density

Q volumetric heat generation, Btu/(ft^3)(sec); J/(m^3)(sec)

Q_o power level defined in eq. (5), Btu/(ft^3)(sec); J/(m^3)(sec)

q heat flux, Btu/(ft^2)(sec); J/(m^2)(sec)

r radius, ft; m

T temperature, ^oR; ^oK

u nondimensional temperature defined in eq. (26)

x nondimensional radius defined in eq. (16)

y nondimensional temperature defined in eq. (15)

z axial position, ft; m

λ constant used in curve fit of concentration

ρ density evaluated at total reactor pressure, atoms/ft^3; atoms/m^3

σ Stefan-Boltzmann constant, Btu/(ft^2)(sec)($^oR^4$); J/(m^2)(sec)($^oK^4$)

τ optical depth defined in eq. (28)

Subscripts:

$\mathbb{c}$ centerline value

e edge value

f property of fuel

j value at jet radius

R radiation

0 reference conditions

Superscripts:

$\bar{}$ mass average

$\vec{}$ vector

$*$ blackbody conditions defined in eq. (6)

$+$ degree of ionization

ANALYSIS

The basic relations governing the radiant heat transfer in a gaseous-fueled nuclear rocket engine will be developed in this section. Conceptually, heat is generated in the nuclear fuel and radiated to the propellant (see fig. 1(a)). Reference 6 showed that if the optical depth of the fuel is large, a diffusion analysis can be used to approximate the radiant heat transport.

If the usual assumptions of local thermodynamic equilibrium and a constant index of refraction equal to one are made, reference 13 shows that a radiant diffusion flux can be defined as

$$\vec{q}_R = -\frac{16\sigma T^3}{3a_R}\nabla T \tag{1}$$

where a_R is a Rosseland mean absorption coefficient and σ is the Stefan-Boltzmann constant. An effective radiative conductivity can then be defined as

$$K_R = \frac{16\sigma T^3}{3a_R} \tag{2}$$

It is assumed that the ordinary thermal conductivity is small compared to this radiative conductivity; therefore, ordinary conduction is neglected. It is also assumed that the convective heat capacity of the fuel region is small compared to the heat conducted away by radiation; therefore, convection is neglected. It is further assumed that the length is much greater than the diameter of the fuel region, and that the region of interest is not near the inlet or exit; therefore, axial heat conduction is neglected.

A typical axial position to be analyzed is shown in figure 1(a) and is enlarged in figure 1(b). The axial position is half way between the entrance and the exit of the reactor. If the axial mixing between the entrance and the exit is not too large this can be considered an average axial position.

At this axial position, the energy equation can be stated as

$$\frac{1}{r}\frac{d}{dr} rK_R \frac{d}{dr} T = -Q \tag{3}$$

where Q is the volumetric heat generation rate. It is assumed that the neutron flux is not attenuated in going through the fuel, so that the volumetric heat generation rate is proportional to the local concentration of fuel atoms.

A quantity of particular importance for nuclear criticality calculations is an average fuel density:

$$\bar{\rho}_f = \frac{\int_0^{r_e} \rho_f C(2\pi r)dr}{\int_0^{r_e} C(2\pi r)dr} \tag{4}$$

The pure fuel density times the mole fraction gives the number of fuel atoms per unit volume; the pure fuel density is evaluated at total reactor pressure. The volumetric heat generation rate can then be given by

$$Q = Q_o \frac{\rho_f}{\bar{\rho}_f} \frac{C}{C_{\text{℄}}} \tag{5}$$

where Q_o is a constant of proportionality determined by the power level of the reactor. Now, let an effective blackbody radiating temperature be defined by

$$T^* \equiv \left(\frac{1}{2\pi r\sigma} \int_0^r (2\pi r)Q\, dr\right)^{1/4} \tag{6}$$

This is the surface temperature necessary to radiate all the heat generated within a black cylinder of radius r. Equation (6) can be combined with equation (5) to give

$$2\pi r\sigma T^{*4} = \frac{Q_o}{C_{\text{℄}}\bar{\rho}_f} \int_0^r \rho_f C(2\pi r)dr \tag{7}$$

Combining equation (7) with equation (4) gives

$$2\pi r_e \sigma T_e^{*4} = \frac{Q_o}{C_{\text{℄}}\bar{\rho}_f}\left(\bar{\rho}_f \int_0^{r_e} C(2\pi r)dr\right) \tag{8}$$

Solving equation (8) for Q_o gives

$$Q_o = \frac{2r_e \sigma T_e^{*4} C_{\text{℄}}}{\int_0^{r_e} C(2r)dr} \tag{9}$$

Reference 8 gives a fuel mole fraction profile for an axial flow system similar to the model in figure 1. The mole fraction profile for this system can be approximated by the following Gaussian type distribution:

$$C = C_{\text{℄}} e^{-\lambda(r/r_j)^2} \tag{10}$$

where λ and $C_{\text{℄}}$ are constants of the curve fit of the numerical calculation given in reference 8. Since equation (10) is Gaussian in form, the exact edge location is not known and will have to be a parameter studied in the calculation.

If equation (10) is substituted into equation (9) and the integration is carried out, the result is

$$Q_o = \frac{2\lambda r_e \sigma T_e^{*4}}{r_j^2\left[1 - e^{-\lambda(r_e/r_j)^2}\right]} = \frac{2\lambda r_e \sigma T_e^{*4}}{r_j^2(1 - C_e/C_{\text{℄}})} \tag{11}$$

Note that in the case where the mole fraction is small at the edge of the fuel, equation (11) can be approximated by

$$Q_o = \frac{2\lambda r_e \sigma T_e^{*4}}{r_j^2} \tag{12}$$

Equations (5) and (11) can be substituted into equation (3), and the first integral can formally be written as

$$K_R \frac{dT}{dr} = -\frac{\dfrac{2\lambda r_e \sigma T_e^{*4}}{r_j^2} \dfrac{1}{r} \displaystyle\int_0^r \frac{\rho_f}{\bar{\rho}_f} \frac{C}{C_{\text{℄}}} r \, dr}{1 - \dfrac{C_e}{C_{\text{℄}}}} \tag{13}$$

where the usual cylindrical boundary condition has been used:

$$\lim_{r \to 0} rK_R \frac{dT}{dr} = 0 \tag{14}$$

The system of equations can be nondimensionalized by using the following transformations:

$$y = \frac{T}{T_e} \tag{15}$$

$$x = \lambda\left(\frac{r}{r_j}\right)^2 \tag{16}$$

$$\frac{d}{dr} = \frac{dx}{dr}\frac{d}{dx} = \frac{2\lambda}{r_j^2} r_j \sqrt{\frac{x}{\lambda}} \frac{d}{dx} \tag{17}$$

Equation (13) then becomes

$$K_R \frac{d}{dx} y = - \frac{\frac{r_e \sigma T_e^{*4}}{2T_e} \frac{1}{x} \int_0^x \frac{\rho_f}{\bar{\rho}_f} \frac{C}{C_{\text{℄}}} dx}{1 - \frac{C_e}{C_{\text{℄}}}} \tag{18}$$

Equation (2) then becomes

$$K_R = \frac{16\sigma T_e^3}{3a_R} y^3 \tag{19}$$

Substituting equation (19) into equation (18) gives

$$\frac{y^3}{a_R}\frac{dy}{dx} = - \frac{\frac{3r_e y_e^{*4}}{32} \frac{1}{x} \int_0^x \frac{\rho_f}{\bar{\rho}_f} \frac{C}{C_{\text{℄}}} dx}{1 - \frac{C_e}{C_{\text{℄}}}} \tag{20}$$

where

$$y^* = \frac{T^*}{T_e} \tag{21}$$

If it is assumed that the absorption of radiation due to the fuel atoms is much greater than that due to the propellant atoms, then the Rosseland mean absorption coefficient will be approximately given by

$$a_R = Ca_{R,f} \tag{22}$$

Figure 2(a) shows Rosseland mean absorption coefficients for the various constituents as calculated in references 4 and 7. It shows that for any temperature the Rosseland mean absorption coefficient is much higher for the nuclear fuel than for the propellant. Although the total Rosseland mean absorption coefficient is not a function of the constituent Rosseland mean absorption coefficients (because various constituents may absorb in other parts of the spectrum), the trend displayed by the constituents in figure 2(a) lends some validity to the approximation used in equation (22). Therefore, equation (22) will be assumed to be correct down to low fuel mole fraction (of the order 0.01).

Figure 2(b) (taken from ref. 4), shows the Rosseland mean absorption coefficient of pure fuel for various pressures. It can be seen that on this log-log plot a straight line is a good curve fit of the Rosseland mean absorption coefficient against temperature. The equation for this curve fit is then

$$a_{R,f} = a_{R,0}\left(\frac{T_0}{T}\right)^m \tag{23}$$

where the subscript 0 refers to reference conditions and m is 2.56.

If equation (15) is substituted into equation (23) and the reference conditions are defined as the edge conditions, the result is

$$a_{R,f} = a_{R,e}y^{-m} \tag{24}$$

If equation (24) is substituted into equation (22) and if the result is substituted into equation (20), the result is

$$y^{m+3}\frac{dy}{dx} = -\frac{3r_e a_{R,e} y_e^{*4}}{32}\frac{C}{x}\int_0^x \frac{\rho_f}{\bar{\rho}_f}\frac{C}{C_{\text{¢}}}\,dx \Bigg/ \left(1 - \frac{C_e}{C_{\text{¢}}}\right) \tag{25}$$

If the transformation

$$u = y^{m+4} \tag{26}$$

is made, the left side of equation (25) becomes a perfect differential:

$$\frac{du}{dx} = -\frac{3(m+4)r_e a_{R,e} y_e^{*4}}{32} \frac{C}{x} \int_0^x \frac{\rho_f}{\bar{\rho}_f} \frac{C}{C_{\mathbb{C}}} dx \Bigg/ \left(1 - \frac{C_e}{C_{\mathbb{C}}}\right) \tag{27}$$

If the definitions

$$\tau_e = a_{R,e} r_e \tag{28}$$

$$A = \frac{3(m+4)C_{\mathbb{C}} \tau_e y_e^{*4}}{32(1 - C_e/C_{\mathbb{C}})} \tag{29}$$

are made and substituted into equation (27) and if equation (10) is used for the value of the mole fraction, the result is

$$\frac{du}{dx} = -A \frac{e^{-x}}{x} \int_0^x \frac{\rho_f}{\bar{\rho}_f} e^{-x} dx \tag{30}$$

Equation (30) can be formally integrated:

$$u = 1 + A \int_x^{x_e} \left(\frac{e^{-x}}{x} \int_0^x \frac{\rho_f}{\bar{\rho}_f} e^{-x} dx \right) dx \tag{31}$$

The value of u at the edge is one, by virtue of the definitions used in equations (15) and (26).

HEAT GENERATION - NOT A FUNCTION OF TEMPERATURE

If the local pure fuel density is not too much different than the average density (i.e., independent of temperature), then the following approximation can be made:

$$\frac{\rho_f}{\bar{\rho}_f} = 1 \tag{32}$$

Substituting equation (32) into equation (31) and performing the indicated integration yield

$$u = 1 + A \sum_{n=1}^{\infty} \frac{(-1)^n (1 - 2^n)(x_e^n - x^n)}{nn!} \tag{33}$$

Figure 3 shows the radial fuel concentration profiles used in the calculation. The more realistic profile, shown as the Gaussian, is compared to an extreme case, the step profile. The step profile is characterized by $\lambda = 0$. Also the approximation given in equation (12) does not apply. Equation (33) applies exactly for the Gaussian profile. The equation for the step profile can be obtained from equation (33) as the limiting expression when $\lambda \to 0$ or

$$u = 1 + A' \left[1 - \left(\frac{r}{r_e} \right)^2 \right] \tag{34a}$$

where

$$A' = \frac{3(m + 4) C_{\text{¢}} \tau_e y_e^{*4}}{32} \tag{34b}$$

If equations (15), (16), and (26) are used, equations (33) and (34a) reduce respectively to

$$T = T_e \left[1 + A \sum_{n=1}^{\infty} \frac{(-\lambda)^n (1 - 2^n)(r_e^{2n} - r^{2n})}{nn!\ r_j^{2n}} \right]^{1/(m+4)} \tag{35}$$

and

$$T = T_e \left\{ 1 + A' \left[1 - \left(\frac{r}{r_j} \right)^2 \right] \right\}^{1/(m+4)} \tag{36}$$

Equations (35) and (36) were used to construct figure 4, where r_e was set equal to r_j in equation (36). The comparison was made for the same power level, thus different neutron fluxes. The average temperature was calculated with the use of equation (4), where the density was assumed to be inversely proportional to the temperature. An explicit value can be given for the step mole fraction profile. Equation (4) can be restated as

$$\frac{1}{\overline{T}_f} = \frac{\int_0^{r_e} \frac{C}{T} 2\pi r \, dr}{\int_0^{r_e} C 2\pi r \, dr} \tag{37}$$

Substituting equation (36) into (37) and using the step mole fraction profile result in

$$\overline{T}_f = A' T_e \frac{m+3}{m+4} \frac{1}{(1 + A')^{\frac{m+3}{m+4}} - 1} \tag{38}$$

If A' is much larger than one and $|(m + 3)/(m + 4)|$ is not close to zero, equation (38) reduces to

$$\overline{T}_f = \frac{m+3}{m+4} T_e A' \frac{1}{m+4} \tag{39}$$

If equations (21), (23), (28), and (34b) are substituted into equation (39),

$$\overline{T}_f = \frac{m+3}{m+4} \left(\frac{3(m+4) r_j C_{¢} a_{R,0} T_0^m T_e^{*4}}{32} \right)^{1/(m+4)} \tag{40}$$

Thus, the variable $\overline{T}_f$, the average temperature of the fuel for the step mole fraction, is a weak function of the edge temperature. The same conclusion can be drawn for equations (35) and (36) for regions not near the edge (as shown in fig. (6)).

Equation (35) was used to construct figures 5 and 6, where again the average density was calculated using equation (37). Figure 5 used the same edge temperature (i.e., the edge temperature set equal to the blackbody radiating temperature) but different edge locations. Figure 6 used the same edge location but different edge temperatures.

HEAT GENERATION - FUNCTION OF TEMPERATURE

In general, the local density does differ from the average density; therefore, equation (32) is not valid. Equation (31) must be solved directly.

It is assumed that the density of the fuel can be treated as though no propellant were present; that is, the presence of the propellant does not change the ionization level of the fuel. Therefore, pure fuel density can be used.

The density of pure fuel is inversely proportional to the temperature times the ratio of the fuel partial pressure to the total pressure. The first term is the result of a volumetric expansion of an ideal gas and the second is due to ionization, and the resulting volume occupied by the electrons. The fuel partial pressure to total pressure ratio was calculated as a function of temperature in reference 9 and is shown in figure 7. For these temperatures the curves can be fitted by a straight line on a log-log plot. The final expression for the pure fuel density can be written as

$$\rho_f = \rho_{f,0}\left(\frac{T_0}{T}\right)^n \tag{41}$$

where subscript zero refers to reference conditions and n is equal to one minus the slope of the straight line curve fit of figure 7 (n is equal to either 1 or 1.79 for 500 atm (5.07×10^7 N/m^2)).

In general, equation (31) can be solved by an iterative technique. First the density over the average density is assumed; then, a temperature distribution is calculated using equation (31). The density over the average density is then calculated using equation (41) on the basis of the new temperature distribution. The entire process is repeated until the average density does not change by more than 10^{-3} percent. Results of this calculation are shown in figures 8 to 11.

DISCUSSION OF RESULTS

The results are presented in terms of local and then average temperatures. First, local fuel temperature is shown as a function of radius. A series of these curves is presented to show how the temperature profile is affected by a fuel mole fraction radial profile, the boundary conditions of edge location and temperature, varying pure fuel density as 1/T, and fuel ionization. After examining the temperature profiles, average fuel temperature is shown as a function of engine thrust level. The effects of a nonuniform mole fraction profile and an arbitrary variation of fuel opacity on the fuel temperature are also presented. Finally, an average fuel temperature calculated with all

effects included is shown for engine thrusts from 100 000 to 1 000 000 pounds (4.45×10^6 to 4.45×10^6 N) and reactor pressures of 100, 500, and 1000 atmospheres (1.01×10^7, 5.07×10^7, 10.1×10^7 N/m^2). All of the results are presented for a specific impulse of 1500 seconds, a value representative of a first-generation gaseous reactor. When they are not parameters or independent variables, engine thrust is 500 000 pounds (2.22×10^6 N) and reactor pressure is 500 atmospheres (5.07×10^7 N/m^2).

The specific impulse and engine thrust determine the values of some other parameters. For example, the specific impulse of 1500 seconds was obtained by assuming a nozzle coefficient of 0.9; that is, 81 percent of the hydrogen enthalpy is converted to thrust. This condition means that the enthalpy out of the engine is 57 500 Btu per pound (1.34×10^8 J/kg). For an engine thrust of 500 000 pounds (2.22×10^6 N), a hydrogen flow rate of 330 pounds per second (150 kg/sec) is required. A reactor power of 20 000 megawatts is required to produce the required enthalpy at this flow rate. Thus, engine thrusts of 10^5 and 10^6 pounds (4.45×10^5 and 4.45×10^6 N) correspond to reactor powers of 4000 and 40 000 megawatts, respectively.

It is assumed that the hydrogen enters the reactor cavity at an enthalpy of 9000 Btu per pound (2.10×10^7 J/kg), (this corresponds to a temperature of about 3000° R), which is obtained as it regeneratively cools the nozzle, moderator, and engine structure. Thus of the 20 000-megawatt total power, 16 800 megawatts is generated in the gaseous fuel and must be radiatively transferred to the hydrogen.

Local Fuel Temperatures

Effect of concentration profile. - Figure 3 shows the two radial distributions of fuel that were investigated. The upper curve represents a cylinder of pure fuel extending out to a radius of 1.6 feet (0.488 m). The lower, Gaussian distribution is a curve fit of a fuel distribution obtained from the computer program described in reference 8. The curve indicates that the centerline mole fraction is 80 atom percent fuel, with the remainder being hydrogen. This curve was fit to the mole fraction profile computed at an axial distance approximately two jet radii from the injection point. For an 8-foot-diameter (2.44-m-diam) reactor cavity, a cavity length of 6 feet (1.83 m), and a uranium jet diameter of 3.2 feet (0.975 m), the axial distance chosen corresponds to the axial midplane of the reactor. Although this particular profile is the result of specific numerical choices, it should be generally representative of the kind of profile that would exist in a gaseous reactor where hydrogen flows coaxially to a centrally located cylinder of fuel. The Gaussian curve is typically encountered in turbulent coflowing jets (ref. 12).

Figure 4 shows the effect of a radial variation of uranium mole fraction on the temperature profile. The upper curve was obtained with a cylinder of pure fuel, while the

lower one corresponds to a mixing case. The blackbody radiating temperature required to radiate 16 800 megawatts from a cylindrical surface 1.6 feet (0.488 m) in radius and 6 feet (1.83 m) long to an environment at absolute zero is 27 000 $^{\circ}$R (15 000 $^{\circ}$K). If mixing reduces the radius of the radiating cylinder by 80 percent (r = 1.28 ft (0.390 m)), then the blackbody radiating temperature necessary to radiate this power increases to 28 800 $^{\circ}$R (16 000° K). The effect of hydrogen dilution of the fuel is to decrease the fuel temperature required to radiate the generated power. This is reasonable, since the high internal temperatures occur because the fuel is too opaque for the heat to be radiated out of the innermost regions. The hydrogen is more transparent than the fuel, so the effect of the fuel dilution is to decrease the opacity down to a limiting value of the propellant opacity near the edge of the fuel region. This permits the internal heat to be radiated more easily, and thus lower temperatures are required. The centerline temperature decreases from 120 000° to 110 000° R (66 700° to 61 100° K), and the mass-weighted average temperature decreases by about 13 percent, 107 000° to 93 000° R (59 400° to 51 700° K).

Effect of fuel boundary conditions. - The boundary values of fuel temperature and radial location would not be independent variables in an actual situation, since they would assume some particular value for given engine operating conditions. In this analytic treatment, however, these values must be prescribed because the model includes only the fuel region. The sensitivity of the calculated fuel temperatures to the choices of these boundary conditions will therefore be investigated. The influence of the location of the "edge" of the fuel will be discussed first; then, the temperature at this edge will be examined.

The location of the outer fuel boundary is obvious for the step mole fraction profile shown in figure 3. It is simply the radius where the fuel mole fraction decreases to zero as a step function. The edge of the fuel is not so easy to locate for the Gaussian profile, since numerically there is always some fuel at any finite radius. Two values of the edge radius were used to determine the sensitivity of the calculated fuel temperatures to this parameter.

For the first case, the fuel region was assumed to end at the same location as for the step profile, that is, at a radius of 1.6 feet (0.488 m). For the Gaussian curve used, the fuel mole fraction at this location is 0.0036 of the centerline value, or an absolute value of about 0.003 atom fraction fuel. At this location, the edge temperature is assumed to be the blackbody temperature necessary to radiate the heat generated within the fuel region, or about 27 000° R (15 000° K). For the second case, the edge of the fuel region is assumed to be at a radius that is 0.8 of the first case, or 1.28 feet (0.390 m). At this radius the mole fraction was about 0.02, and it was assumed that this was low enough value to neglect the fuel outside this radius.

Figure 5 shows the radial temperature profile for these two cases. The only

significant effect of the edge location is on the fuel temperatures near the edge. This has very little influence on the average fuel temperature because the amount of fuel near the edge is low due to the low fuel mole fraction. For the case illustrated in figure 5, a variation of 20 percent in the radius of the edge caused a change of less than 2 percent in the average fuel temperature.

Since the internal temperatures seem to be insensitive to the exact edge location and since the mole fraction of fuel has decreased to a small value at a radius of 1.28 feet (0.390 m), a radius of 1.28 feet (0.390 m) is used as the edge of the fuel for the remaining calculations.

The significance of the location of the edge of the fuel is that this is where a boundary value of temperature is assigned. A priori, the internal fuel temperatures are influenced by the value chosen for the edge temperature. If there is no back radiation to the fuel from the surroundings, and if the fuel region is many radiation mean free paths thick, then the edge temperature would be essentially the blackbody temperature necessary to radiate the energy that is internally generated. Back radiation would raise the edge temperature above this effective blackbody radiating temperature.

Figure 6 shows radial temperature profiles for ratios of edge to blackbody temperatures of 1, 2, and 3. For an edge to blackbody temperature radio of 2, the average fuel temperature is 2 percent higher than for a ratio of 1. A ratio of 3 causes an increase of 7 percent. Thus as long as the edge temperature does not approach the average temperature, estimates of average fuel temperature should be insensitive to the boundary value for the high-power densities of interest here.

The actual case, which is beyond the scope of this report, would have to consider additional effects. First, the opacity of the hydrogen itself could be considered; second, the actual fuel edge temperature would be influenced by the spectral nature of both the fuel emission and the hydrogen absorption coefficient; and third, the fuel edge would also be influenced by additional modes of energy transport not considered here - for example, electron conduction and turbulence.

It is not possible in the present analysis to calculate the fuel edge temperature, because it is an input parameter. Since a seed material must be added to the hydrogen to increase its opacity at low temperatures, an estimate can be made of the back radiation effect due to the temperature rise of the seeded hydrogen that surrounds the fuel region (neglecting the hydrogen opacity). From figure 2(a), it is estimated that a representative absorption coefficient of the seeded hydrogen is 4 ft^{-1} (13.1 m^{-1}). Thus one optical mean free path is 0.25 foot (7.66 cm). For a fuel radius of 1.6 feet (0.488 m) and a reactor cavity radius of 4 feet (1.22 m), one-sixteenth of the total hydrogen flow rate is flowing in an annular sheath, around the fuel region, that is one radiation mean free path thick.

All of the energy that is radiated from the fuel region enters this surrounding layer of hydrogen. In order to estimate the temperature to which this hydrogen layer is heated,

it will be assumed that 63 percent (1 - 1/e) of the entering energy is absorbed. It is also assumed that half of this absorbed energy is radiated back toward the fuel region; the other half is radiated outward into the remainder of the hydrogen. With these assumptions it can be shown that, for the 20 000-megawatt engine being considered, the hydrogen in the 0.25-foot (7.66-cm) layer will reach a temperature of 13 500° R (7500° K) by the time it is halfway through the reactor. The ratio of fuel-edge-to-effective-blackbody temperature necessary to overcome the back radiation from this temperature is 1.02.

From the results shown in figure 6, two conclusions are indicated. First, the calculated average fuel temperature is relatively insensitive to the value of the boundary temperature assigned at some radius near the outer edge. Second, the fuel edge temperature will not be increased significantly over the effective blackbody temperature because of back radiation from the seed material in the surrounding hydrogen.

The general conclusion of the results shown in figures 5 and 6 is that average fuel temperatures are relatively insensitive to both the precise location of the fuel edge and to the value of temperature that is assigned at that point. All of the remaining results to be presented in this report will be for the Gaussian mole fraction distribution (unless otherwise noted) shown in figure 3, a fuel region radius of 1.28 feet (0.390 m), and an edge temperature necessary to radiate the reactor power as a blackbody, or about 28 800° R (16 000° K).

Effect of fuel perfect gas density variation and ionization. - There are at least two other factors which tend to produce radial variations in the volumetric heat source distribution. One of these factors is the perfect gas density variation of the fuel, 1/T, due to the temperature profile. Thus, the high centerline temperatures produce proportionally lower concentrations, and this tends to shift the power generation toward the outer, lower temperature fuel regions. The second effect to be considered is that due to fuel ionization. This also tends to reduce the volumetric heat source strength in regions where temperatures are highest. The degree of fuel ionization at a given temperature is pressure dependent, but not strongly so. Figure 7 shows the ratio of uranium particle (atom or ion) partial pressure to the total pressure as a function of temperature. This ratio is less than 1 because of the electron pressure. The curves of figure 7 were computed by the method of reference 9 modified to include charged particles. Uranium ionization potentials used in this calculation were provided by J. T. Waber, D. Liberman, and D. T. Cromer of Los Alamos Scientific Laboratory. References 10 and 11 describe related work. The ionization potentials used in this investigation are listed in table I. These ionization potentials were calculated by Dr. J. T. Waber (LASL) about May 27, 1966, using self-consistent-field Dirac wave functions calculated with two-thirds of Slater's exchange potential except at large radii, where the Latter "tail" correction was applied to the exchange potential.

TABLE I. - IONIZATION POTENTIALS

OF URANIUM

Atom or ion	Ionization potential with only spin-orbit splitting (theoretical)	
	eV	J
U	4.42	7.08×10^{-19}
U^{+}	11.46	18.4
U^{++}	17.94	28.7
U^{3+}	31.14	49.9
U^{4+}	46.03	73.8
U^{5+}	61.82	99.1
U^{6+}	87.93	141
U^{7+}	101.1	162
U^{8+}	115.0	184
U^{9+}	128.9	207
U^{10+}	157.9	253
U^{11+}	178.5	286

The effects of fuel density varying as 1/T and fuel ionization on the temperature profile are shown in figure 8. The upper curve on figure 8 is the lower one shown in figure 4; it was calculated using the Gaussian mole fraction profile. The middle curve of figure 8 includes the effects of both mole fraction profile and density variation due to temperature, but not ionization. The lower curve includes all three effects. These results show that the density variation and ionization of fuel both reduce the near-centerline temperatures, but that the effect is a relatively small one. For the case illustrated in figure 8, the combined effect was to reduce the average fuel temperature by about 7 percent. Neither effect is very significant, and both have the same general influence - that is, to decrease the central region temperatures about 3 percent.

Average Fuel Temperatures as a Function of Thrust

Effect of mole fraction profile. - As was illustrated in figure 4, a radially decreasing fuel mole fraction reduces both local and average fuel temperatures as compared to those for a step fuel mole fraction profile. Figure 9 shows a comparison of average fuel temperatures for the two profiles for engine thrust levels from 10^5 to 10^6 pounds (4.45×10^5 to 4.45×10^6 N). Over this range of engine thrust, the Gaussian mole fraction profile yields average fuel temperatures that are from 10 to 15 percent lower than those calculated using a step mole fraction profile. The curves of figure 9 do not include the effects of density or ionization of the fuel.

Effect of fuel absorption coefficient. - In addition to the heat source strength and distribution and the boundary conditions, fuel temperature is affected by the value used for the absorption coefficient. In the diffusion approximation, for example, the conductivity of the gas is inversely proportional to the absorption coefficient. Because the uranium atom is a complicated one, future modifications in the theory, new input quantities, or experimental measurements may give different values for the absorption coefficient than those used in this study. It is therefore of interest to determine the sensitivity of the present results to the numerical values used for the absorption coefficient. It is assumed that the statistical model used in reference 4 is as good a representation of the uranium atom as is presently available. Future modifications of the theory will probably take the form of new values of input quantities such as ionization potentials and line spacing. These quantities in general will affect the absolute level of the absorption coefficient more than the functional temperature dependence. The absolute level of the absorption coefficient given in figure 2(b) for a pressure of 500 atmospheres (5.07×10^7 N/m^2) was parametrically varied keeping the slope constant.

Average fuel temperatures were calculated using an absorption coefficient from figure 2(b), a value 10 times as large, and a value 0.1 as large. The results are shown in figure 10. All of these curves are for a Gaussian mole fraction profile. At a thrust level of 500 000 pounds (2.22×10^6 N), a variation of a factor of 10 in the absorption coefficient causes a 35-percent change in the average fuel temperature. An increase in the absorption coefficient causes an increase in the average fuel temperature. The general conclusion here is that to estimate average fuel temperatures within ±10 percent, the absorption coefficient has to be known within about a factor of 2.

Effect of reactor pressure. - All of the preceeding calculations were at a reactor pressure of 500 atmospheres (5.07×10^7 N/m^2). Reactor pressure level affects the average fuel temperature because the absorption coefficient is almost proportional to it, as indicated in figure 2(b). The effect of an increase in pressure is to increase the absorption coefficient and to decrease the degree of ionization; both of these changes cause an increase in fuel temperature.

Average fuel temperatures as a function of engine thrust were computed for reactor pressures of 100, 500, and 1000 atmospheres (1.01×10^7, 5.07×10^7, and 10.1×10^7 N/m^2). These values are shown in figure 11 for engine thrusts up to 1 000 000 pounds (4.45×10^6 N) at a specific impulse of 1500 seconds. The curves were calculated using (1) the Gaussian distribution of fuel given in figure 3, (2) an edge temperature of the blackbody radiating temperature, at a fuel edge radius of 1.28 feet (0.390 m), (3) fuel ionization as shown in figure 7, and (4) perfect gas density variation of the fuel.

Figure 11 shows that reactor pressure has a significant effect on the average fuel temperature. For example, at an engine thrust of 500 000 pounds (2.22×10^6 N), the average fuel temperature increases from 71 000° R (39 400° K) at 100 atmospheres

(1.01×10^7 N/m^2) pressure to 93 000° R (51 700° K) at 1000 atmospheres (10.1×10^7 N/m^2). Overall, figure 11 indicates that gaseous reactor fuel average temperatures range from a low of 55 000° R (30 500° K) at a pressure of 100 atmospheres (1.01×10^7 N/m^2) and a thrust of 10^5 pounds (4.45×10^5 N), up to a high of 110 000° R (61 100° K) at a pressure of 1000 atmospheres (10.1×10^7 N/m^2) and a thrust of 10^6 pounds (44.5×10^5 N).

All of these numbers and conclusions are for the situation where the reactor power generated in the gaseous fuel is transferred to the seeded hydrogen entirely by thermal radiation. Lower fuel temperatures will exist if a significant amount of the energy is transferred by some other mechanism, such as turbulent heat transport or electron heat conduction. These processes are not included here, and the estimates of fuel temperature in figure 11 will have to be revised downward if future information shows conduction or convection to be important processes.

SUMMARY OF RESULTS

A one-dimensional diffusion analysis has been made of the thermal radiation heat transfer in a gaseous-core nuclear rocket engine. The specific reactor analyzed had a cavity length of 6 feet (1.83 m), a cavity diameter of 8 feet (2.44 m), and a fuel diameter of 3.2 feet (0.975 m). The analysis was used to calculate radial temperature profiles and average temperatures in the fuel region. Parametric calculations were carried out to determine the influence on local and average fuel temperatures of (1) the location of the fuel edge or boundary, (2) the boundary value of temperature at the fuel edge, (3) a decreasing radial Gaussian fuel mole fraction profile, (4) the pure fuel partial density varying inversely with temperature, (5) fuel ionization, (6) the magnitude of the fuel absorption coefficient, (7) reactor pressure, and (8) engine thrust.

All of the calculations were carried out for a specific impulse of 1500 seconds. This corresponds to a hydrogen enthalpy of 57 500 Btu per (1.34×10^8 J/kg) for a nozzle velocity coefficient of 0.9. Most of the calculations were made for a reactor pressure of 500 atmospheres (5.07×10^7 N/m^2) and an engine thrust of 500 000 pounds (2.22×10^6 N); this latter corresponds to 330 pounds per second (150 kg/sec) of hydrogen and a reactor power of 20 000 megawatts. A final set of average fuel temperatures are presented for reactor pressures of 100, 500, and 1000 atmospheres (1.01×10^7, 5.07×10^7, 10.1×10^7 N/m^2) and engine thrusts from 10^5 to 10^6 pounds (4.45×10^5 to 44.5×10^6 N). The study yielded the following results for the 20 000-megawatt, 1500-second engine:

1. When changing from a radial constant fuel mole fraction (step profile) to a radial decreasing fuel mole fraction (Gaussian profile), the average fuel temperature decreased

from 107 000° to 92 500° R (59 400 to 51 400° K).

2. When the edge location was changed from 1.28 to 1.6 feet (39.0 to 48.8 cm), the average fuel temperature increased from 92 500° to 93 000° R (51 400° to 51 700° K) for the 20 000-megawatt, 1500-second engine.

3. When the edge temperature was changed from 28 800° to 57 600° R (16 000° to 32 000° K) and then to 86 400° R (48 000° K), the average fuel temperature increased from 92 500° to 94 500° R (51 400° to 52 500° K) and then to 103 500° R (57 500° K), respectively.

4. When the fuel density variation was changed from being temperature independent to that of a perfect gas variation (1/T) and then to a variation including fuel ionization, the average fuel temperature decreased from 92 500° to 91 500° R (51 400° to 50 800° K) and then to 89 000° R (49 400° K), respectively.

5. When the fuel absorption coefficient of the fuel was changed from its initial value to one-tenth of the initial value and then to ten times the initial value, the average fuel temperature decreased from 89 000° to 63 000° R (49 400° to 35 000° K) and then increased to 126 000° R (70 000° K) respectively.

6. When the pressure level of the reactor was changed from 500 to 100 atmospheres (5.07×10^7 to 1.01×10^7 N/m^2) and then to 1000 atmospheres (10.1×10^7 N/m^2), the average fuel temperature decreased from 89 000° to 71 000° R (49 400° to 39 500° K) and then to 96 000° R (53 400° K).

Overall, gaseous reactor fuel temperatures ranged from 55 000° R (30 500° K) at a pressure of 100 atmospheres (1.01×10^7 (N/m^2) and a thrust of 10^5 pounds (4.45×10^5 N), to 110 000° R (61 100° K) at a pressure of 1000 atmospheres (10.1×10^7 N/m^2) and a thrust of 10^6 pounds (4.45×10^5 N). This and all preceding conclusions apply to a reactor in which the energy transfer is solely by thermal radiation. Lower fuel temperatures will exist if some additional mechanism such as turbulent transport or electron conduction is significant.

Lewis Research Center,
National Aeronautics and Space Administration,
Cleveland, Ohio, March 29, 1967,
122-28-02-17-22.

REFERENCES

1. Cooper, Ralph S., Compiler: Proceedings of an Advanced Nuclear Propulsion Symposium. Rep. No. LA-3229-MS, Los Alamos Scientific Lab., June 1965.
2. Ragsdale, Robert G.; and Einstein, Thomas H.: Two-Dimensional Gray-Gas Radiant Heat Transfer in a Coaxial-Flow Gaseous Reactor. NASA TN D-2124, 1964.
3. Kascak, Albert F.: Coaxial Flow Radiation Heat Transfer Analysis. Proceedings of an Advanced Nuclear Propulsion Symposium, Ralph S. Cooper, Compiler. Rep. No. LA-3229-MS, Los Alamos Scientific Lab., June 1965, pp. 208-221.
4. Krascella, N. L.: Theoretical Investigation of the Opacity of Heavy-Atom Gases. Rep. No. D-910092-4 (NASA CR-69001), United Aircraft Corp., Sept. 1965.
5. McLafferty, G. H.; Michels, H. H.; Lathem, T. S.; and Roback, R.: Analytical Study of Hydrogen Turbopump Cycles for Advanced Nuclear Rockets. Rep. No. D-910093-19 (NASA CR-68988), United Aircraft Corp., Sept. 1965, App. 1.
6. Howell, John R.: Radiative Interactions Between Absorbing-Emitting and Flowing Media with Internal Energy Generation. NASA TN D-3614, 1966.
7. Krascella, N. L.: Tables of the Composition, Opacity, and Thermodynamic Properties of Hydrogen at High Temperatures. NASA SP-3005, 1963.
8. Weinstein, Herbert; and Todd, Carroll A.: Analysis of Mixing of Coaxial Streams of Dissimilar Fluids Including Energy-Generation Terms. NASA TN D-2123, 1964.
9. Zeleznik, Frank J.; and Gordon, Sanford: A General IBM 704 or 7090 Computer Program for Computation of Chemical Equilibrium Compositions, Rocket Performance, and Chapman-Jouguet Detonations. NASA TN D-1454, 1962.
10. Liberman, D.; Waber, J. T.; and Cromer, Don T.: Self-Consistent-Field Dirac-Slater Wave Functions for Atoms and Ions. I. Comparison with Previous Calculations. Phys. Rev., vol. 137, no. 1A, Jan. 4, 1965, pp. 27-34.
11. Cowan, R. D.; Larson, A. C.; Liberman, D.; Mann, J. B.; and Waber, J.: Statistical Approximation for Exchange in Self-Consistent-Field Calculations of the Ground State of Neutral Argon. Phys. Rev., vol. 144, no. 1, Apr. 8, 1966, pp. 5-7.
12. Hinze, J. O.: Turbulence; an Introduction to Its Mechanism and Theory. McGraw-Hill Book Co., Inc., 1959, p. 417.
13. Hirschfelder, Joseph O.; Curtiss, Charles F.; and Bird, R. Byron: Molecular Theory of Gases and Liquids. John Wiley and Sons, Inc., 1954, p. 724.

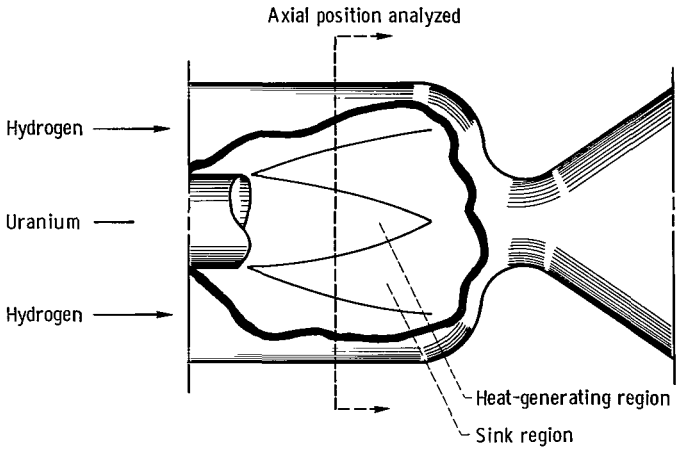

(a) Engine concept. Heat is generated in the fissioning fuel and is radiated to the propellant.

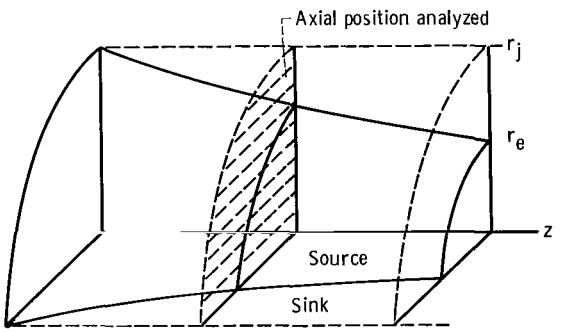

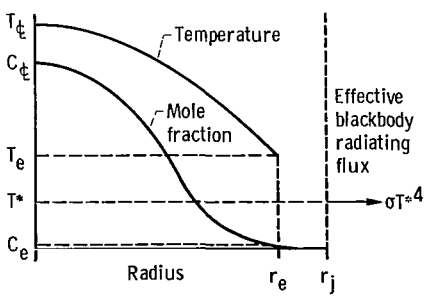

(b) Analytical model showing nomenclature.

Figure 1. - Heat-transfer system.

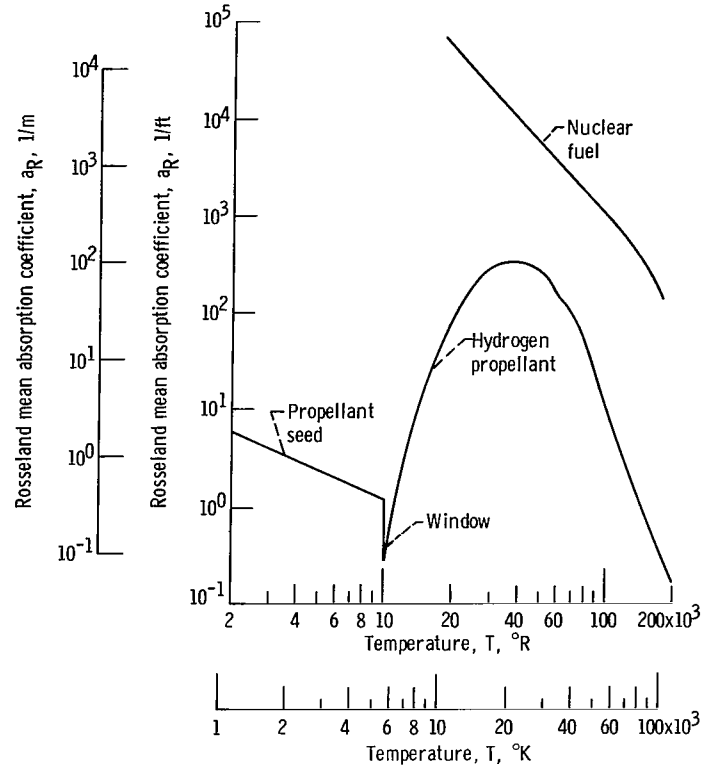

(a) All species at a pressure of 500 atmospheres (5.07×10^7 N/m^2).

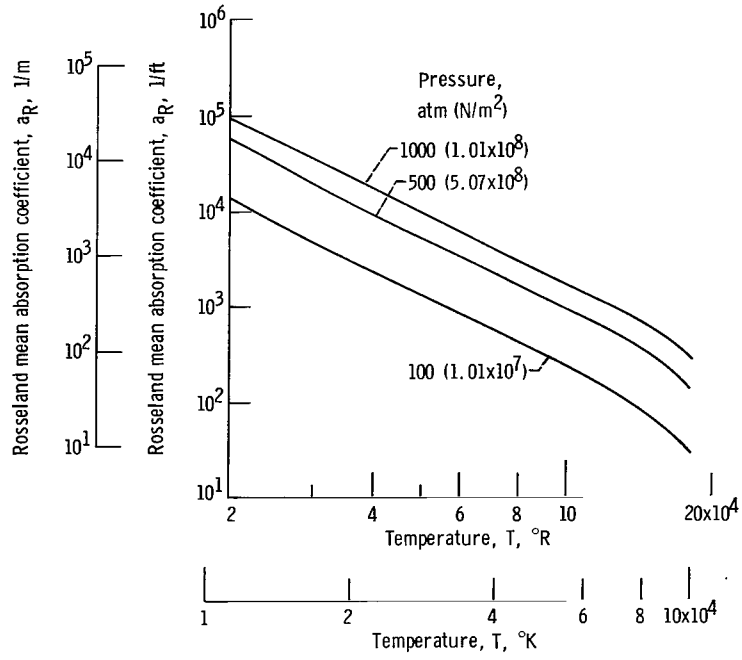

(b) Uranium.

Figure 2. - Absorption coefficients.

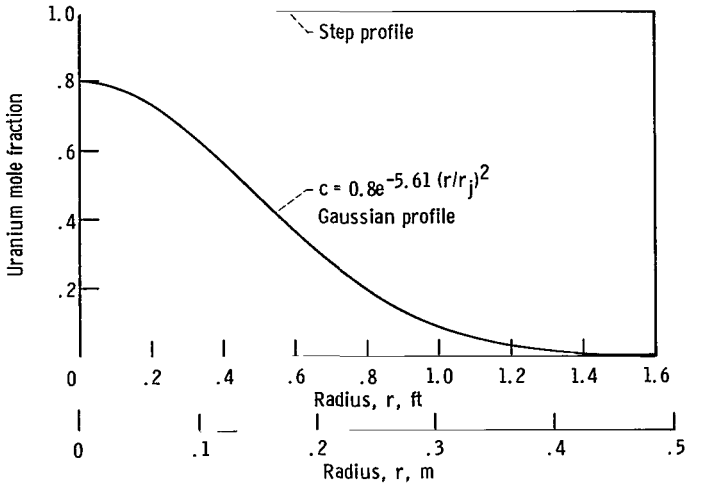

Figure 3. - Mole fraction profile at reactor midplane.

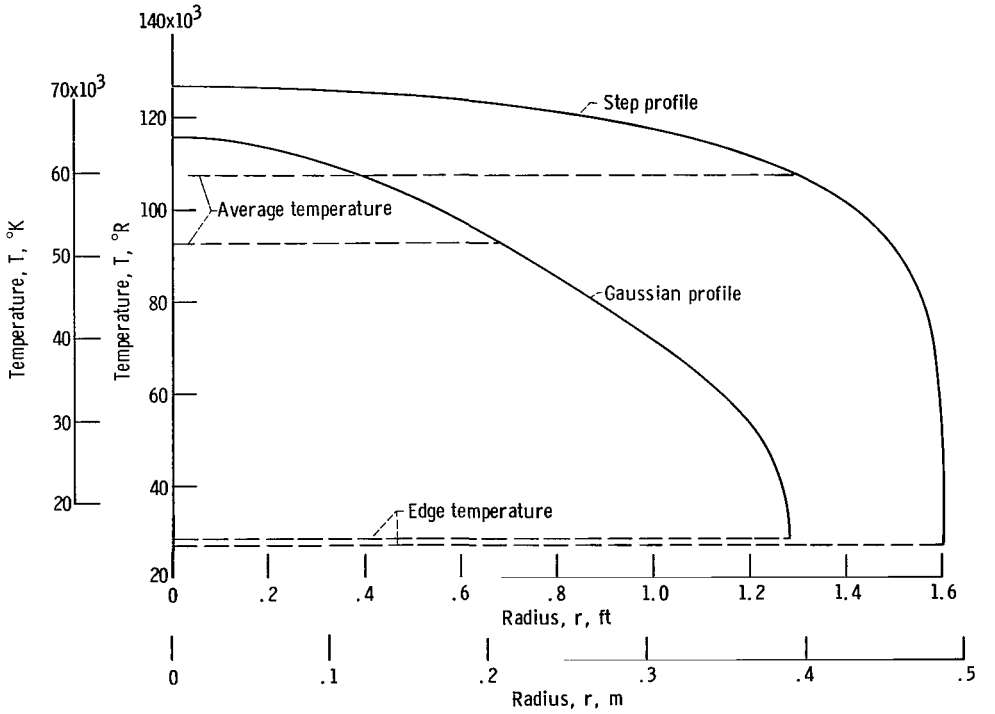

Figure 4. - Effect of varying mole fraction on fuel temperature profile. Reactor pressure, 500 atmospheres (5.07×10^7 N/m^2); thrust, 500 000 pounds (2.22×10^6 N).

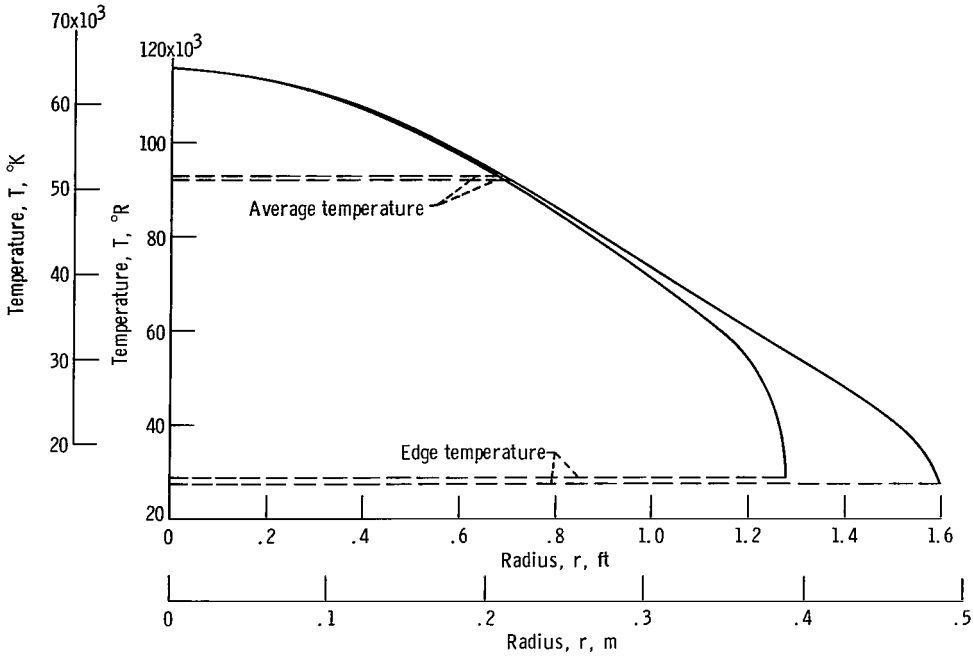

Figure 5. - Effect of edge location on fuel temperature profile with Gaussian mole fraction profile. Pressure, 500 atmospheres (5.07×10^7 N/m^2); thrust, 500 000 pounds (2.22×10^6 N).

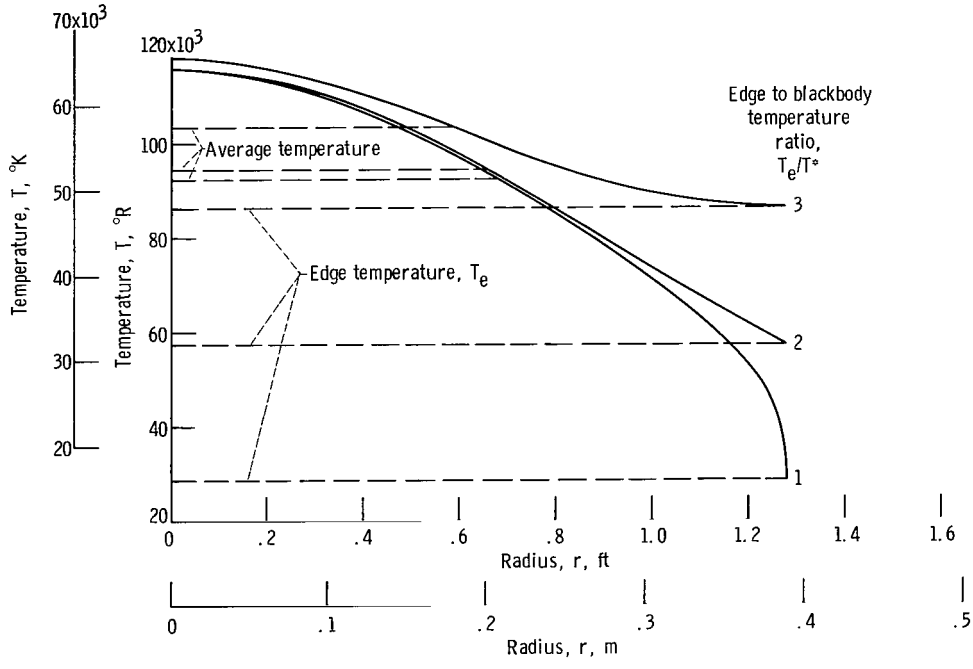

Figure 6. - Effect of varying edge temperature on fuel temperature profiles with Gaussian mole fraction profile. Pressure, 500 atmospheres (5.07×10^7 N/m^2); thrust, 500 000 pounds (2.22×10^6 N).

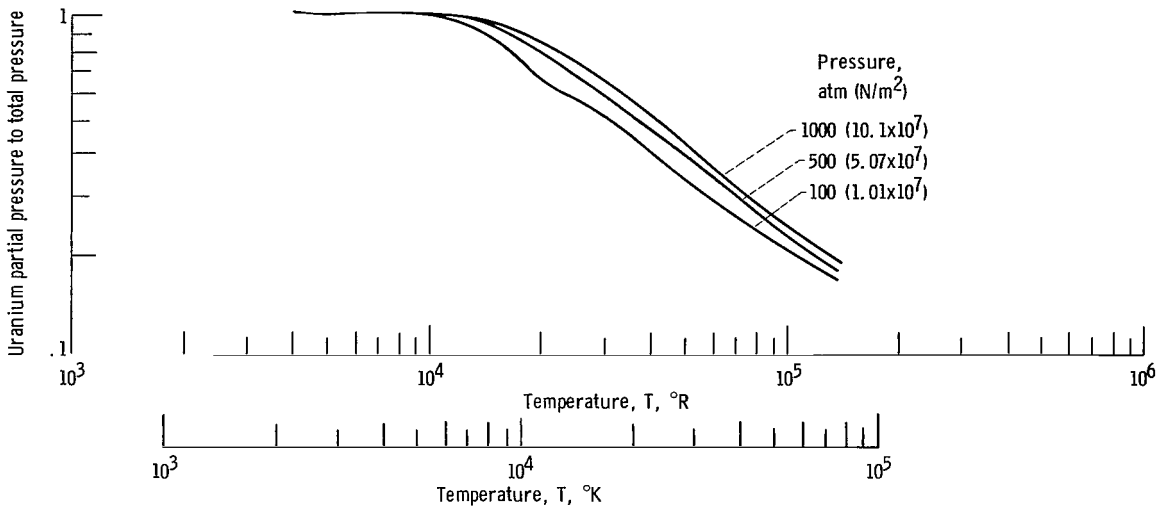

Figure 7. - Uranium partial pressure to total pressure as function of temperature.

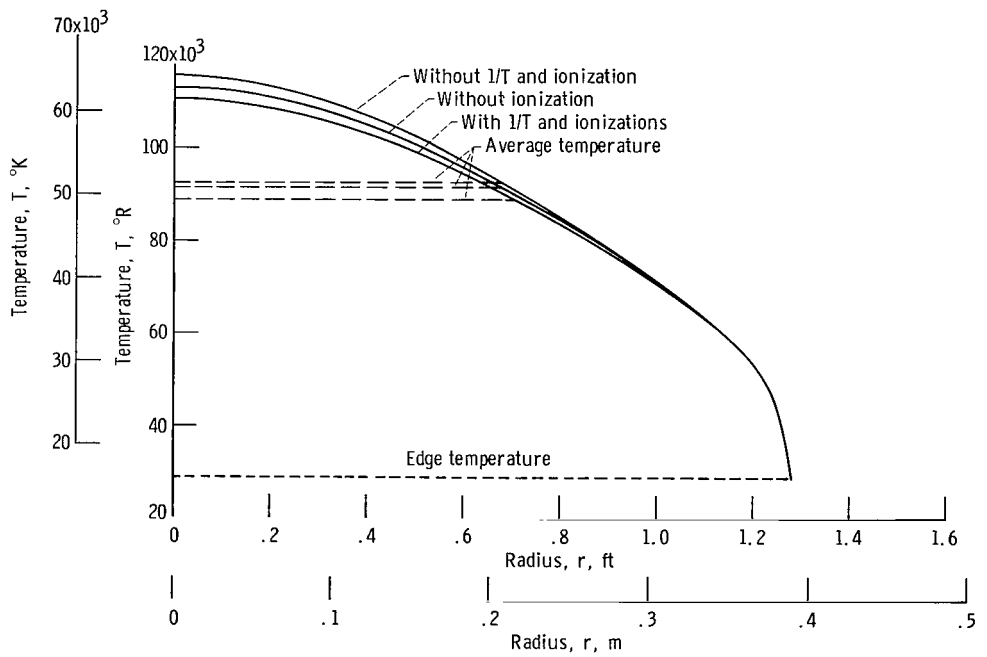

Figure 8. - Effect of volumetric expansion (1/T) and ionization on radial temperature profile with Gaussian mole fraction profile. Pressure, 500 atmospheres (5.07×10^7 N/m^2); thrust, 500 000 pounds (2.22×10^6 N).

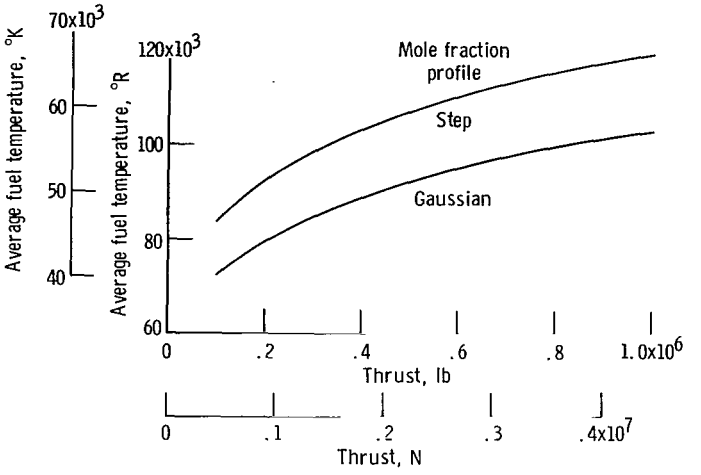

Figure 9. - Variation of average fuel temperature with thrust level for step and Gaussian fuel mole fraction profiles. Pressure, 500 atmospheres (5.07×10^7 N/m^2); specific impulse, 1500 seconds.

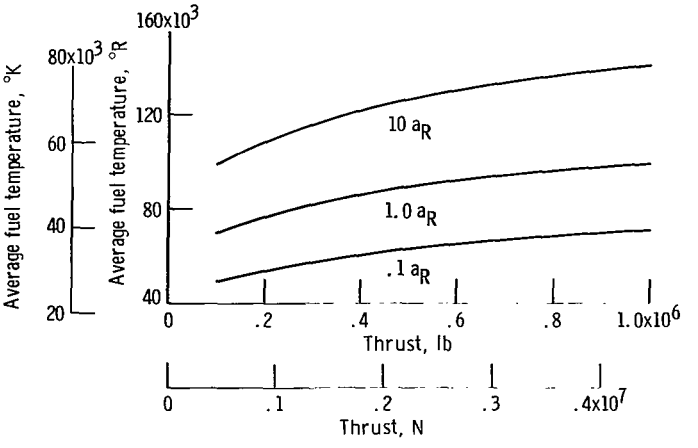

Figure 10. - Variation of average fuel temperature with thrust level for arbitrary changes in Rosseland mean absorption coefficient a_R.

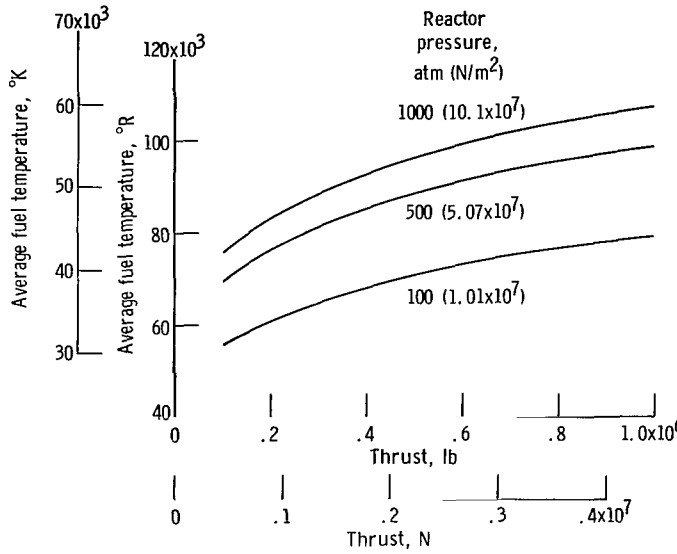

Figure 11. - Effect of thrust level on average fuel temperatures in gaseous reactor for Gaussian mole fraction including effects of fuel density variations and reactor pressures of 100, 500, and 1000 atmospheres. Specific impulse, 1500 seconds.

"The aeronautical and space activities of the United States shall be conducted so as to contribute . . . to the expansion of human knowledge of phenomena in the atmosphere and space. The Administration shall provide for the widest practicable and appropriate dissemination of information concerning its activities and the results thereof."

—NATIONAL AERONAUTICS AND SPACE ACT OF 1958

NASA SCIENTIFIC AND TECHNICAL PUBLICATIONS

TECHNICAL REPORTS: Scientific and technical information considered important, complete, and a lasting contribution to existing knowledge.

TECHNICAL NOTES: Information less broad in scope but nevertheless of importance as a contribution to existing knowledge.

TECHNICAL MEMORANDUMS: Information receiving limited distribution because of preliminary data, security classification, or other reasons.

CONTRACTOR REPORTS: Scientific and technical information generated under a NASA contract or grant and considered an important contribution to existing knowledge.

TECHNICAL TRANSLATIONS: Information published in a foreign language considered to merit NASA distribution in English.

SPECIAL PUBLICATIONS: Information derived from or of value to NASA activities. Publications include conference proceedings, monographs, data compilations, handbooks, sourcebooks, and special bibliographies.

TECHNOLOGY UTILIZATION PUBLICATIONS: Information on technology used by NASA that may be of particular interest in commercial and other non-aerospace applications. Publications include Tech Briefs, Technology Utilization Reports and Notes, and Technology Surveys.

Details on the availability of these publications may be obtained from:

SCIENTIFIC AND TECHNICAL INFORMATION DIVISION

NATIONAL AERONAUTICS AND SPACE ADMINISTRATION

Washington, D.C. 20546